ОБЪЕДИНЕННЫЙ
ИНСТИТУТ
ЯДЕРНЫХ
ИССЛЕДОВАНИЙ

Дубна

E13-95-241

S.V.Uchaikin

SYSTEM FOR MEASUREMENTS OF THE CURRENT-PHASE RELATION IN SUPERCONDUCTING WEAK LINKS

Submitted to the Third Symposium of Low Temperature Electronics and High Temperature Superconductivity, Reno, Nevada, 22—27 May 1995

1995

INTRODUCTION

The performances of the superconducting weak links are defined by their current-phase relation in many aspects. In general the Cooper pair current through the weak link I_P can be written in the form:

$$I_P = \sum_{m=1}^{\infty} I_m \sin m\varphi, \tag{1}$$

where $\varphi-$ is the phase difference of the order parameter across the Josephson junction. In case the high quality Josephson junction parts with $m > 1$ are ignored and the current-phase relation is sinusoidal:

$$I_P(\varphi) = I_C \sin\varphi, \tag{2}$$

where I_C- is the critical current of the weak link. The equation [2] is included in the basic equation of the RSJ-model (1,2) for the current flowing through the weak link:

$$I = I_P(\varphi) + \frac{\hbar}{2e}\frac{1}{R_F}\frac{d\varphi}{dt} + \frac{\hbar}{2e}C\frac{d^2\varphi}{dt^2} + I_F, \tag{3}$$

where R_F- is the normal resistance of the junction; $C-$ its capacitance; $\hbar-$ Planck's constant, $e-$ the charge of the electron; I_F- is the fluctuation current produced by R_F.

The nonsinusoidal current-phase relation may lead to the violation of the RSJ-model and complication of the weak link behavior. It may cause a dramatical degradation of the performances based on the Josephson effect devices. In case of SQUIDs it may be the reason of the SQUID intrinsic noise increasing (3). That is why it is desirable to investigate this relation to optimize the technological process of the Josephson devices manufacturing.

METHOD OF THE MEASUREMENTS

There are various methods to investigate $I_P(\varphi)$. At present the Josephson devices are used at the temperature of 100 K and more, and it is important to choose the method for every case. The Vincent-Deaver approach for indirect measurements proposed in (4) is suitable over the wide temperature range and can be used for the conventional and high $-T_C$ superconductor weak link estimations (5,6). This method consists in measuring a small signal impedance of the weak links incorporated in the rf SQUIDs operating in the strongly nonhysteretic mode. A model of the weak link embedded in a superconducting ring coupled to the tank circuit $L_T C_T$, is shown in Fig.1 (7). As usual we neglect the Josephson junction capacitance. Phase dependent inductor $\mathcal{L}(\varphi)$ of the weak link is connected with the pair current I_P flowing through it:

$$\mathcal{L}(\varphi) = \frac{\hbar}{2e}\left(\frac{dI_P(\varphi)}{d\varphi}\right)^{-1} \qquad [4]$$

Thus, we are able to calculate the current phase relation $I_P(\varphi)$ to investigate the influence of $\mathcal{L}(\varphi)$ on the tank curcuit.

The calculations are carried out as follows (7). L_T is measured before hand. If L_T is known, values R_T and C_T may be defined from the measurements of the tank resonance frequency ω_0 and quality factor Q_0. Mutual inductance M between L_T and the SQUID loop inductance L is determined by measuring of the variation period of the tank voltage V_T when L_T is supplied with dc current I_{DC}. Then effective inductance L_{EFF} and resistance R_{EFF} are calculated at different values of externally applied flux Φ_{DC} using [5] and [6] to measure quality factor Q and resonance frequency ω :

$$Q = \frac{\omega \cdot L_{EFF}}{R_{EFF}} \qquad [5]$$

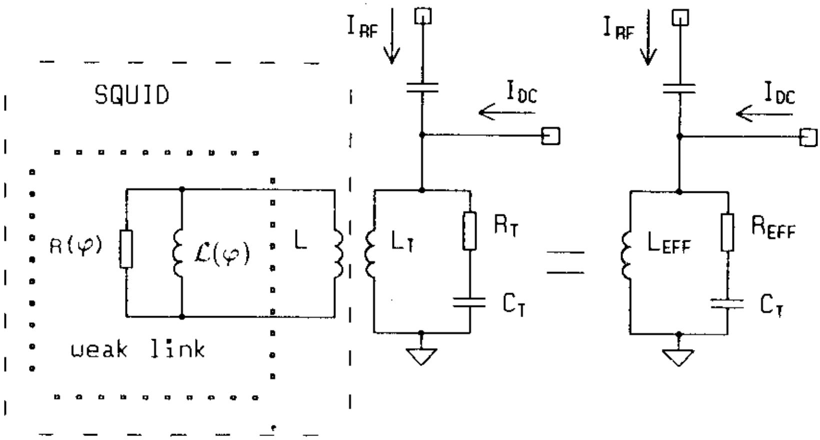

Figure 1. Diagram of weak link in superconducting ring coupled. to tank cureuit.

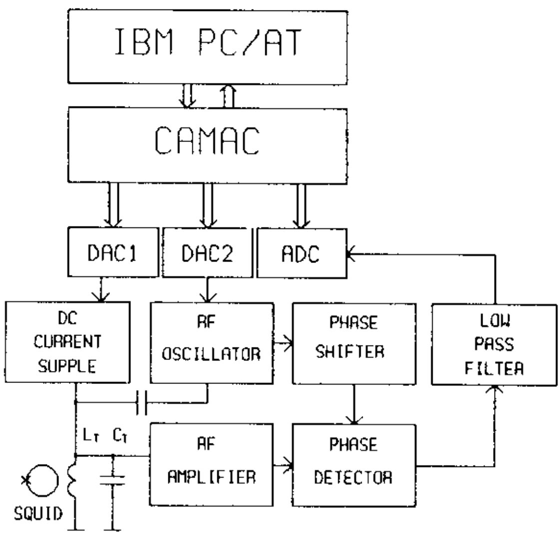

Figure 2. Schematic diagram of experimental setup.

$$\omega = \sqrt{\frac{1}{L_{EFF}C_T} - \left(\frac{R_{EFF}}{2L_{EFF}}\right)^2} \qquad [6]$$

Substituting all the above values in equations [7] and [8] one can obtain $\mathcal{L}(\Phi_{DC})$ and $R(\Phi_{DC})$:

$$\mathcal{L} = \frac{(R_{EFF} - R_T)^2L^2 + \omega^2[M^2 + (L_{EFF} - L_T)L]^2}{-\omega^2(L_{EFF} - L_T)[M^2 + (L_{EFF} - L_T)L] - (R_{EFF} - R_T)^2L}, \qquad [7]$$

$$R = \frac{(R_{EFF} - R_T)^2L^2 + \omega^2[M^2 + (L_{EFF} - L_T)L]^2}{(R_{EFF} - R_T)M^2}. \qquad [8]$$

The transfer to argument φ can be obtained by means of numerical integration with relation [9]:

$$\varphi(\Phi_{DC}) = \int_0^{\Phi_{DC}} \left[1 + \frac{L}{\mathcal{L}(\Phi_{DC})}\right]^{-1} d\Phi_{DC}. \qquad [9]$$

Then the current phase relation is calculated with equation [4].

SYSTEM DESIGN

In this paper a system for these measurements is described. Since these investigations have required many measurements, we decided to make them automatic. The functional diagram of the computer-controlled system is given in Fig.2. The system includes a voltage controlled dc current supply, a voltage tuned rf oscillator, a phase shifter, a wideband rf amplifier with the first cooled stage operating at $4-300\ K$, a phase-sensitive detector, a low-pass filter, two digital-analog 12 bit converters (DAC) and an analog-digital 12 bit converter (ADC).

The amplifier (Fig.3) utilizes a cooled GaAs transistor V1 as the input device in a cascode configuration. The first and second stages of the cascode are constructed with different sources to select the best transistor regimes. The load of the second stage is the cascode in analogy with (8). The cascode amplifier is followed by two stages of emitter followers to provide the 50Ω impedance drive for the output amplifiers. Two silicon bipolar 50Ω amplifiers are used for the output stages (INA-02184, Avantek). Two types of GaAs transistors were tested as the cooled amplifier – AP354G-2 (NPO "Saturn", Kiev, Ukraine) and ATF-10136. The white noise level was less than 0.6 $nV/Hz^{1/2}$ and 0.5 $nV/Hz^{1/2}$ at 4.2 K, accordingly. The frequency response is flat in the range between 10 and 80 MHz.

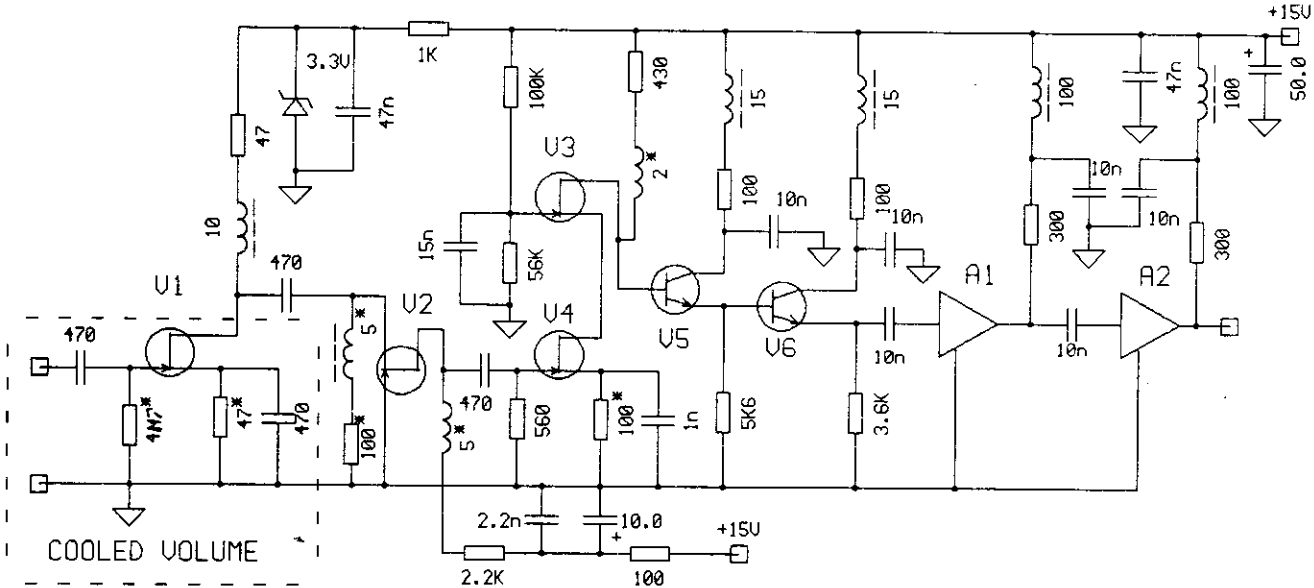

Figure 3. Curcuit diagram of the rf amplifier. $V1$– see the text; $V2 \div V4$– KP307; $V5, V6$– KT3120; $A1, A2$– INA-02184.

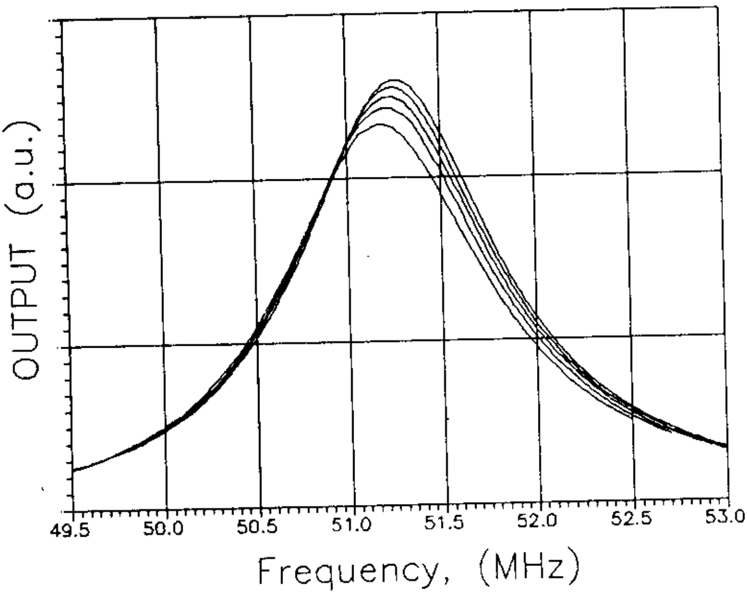

Figure 4. Amplitude-to-frequency curves of the tank curcuit at various Φ_{DC}.

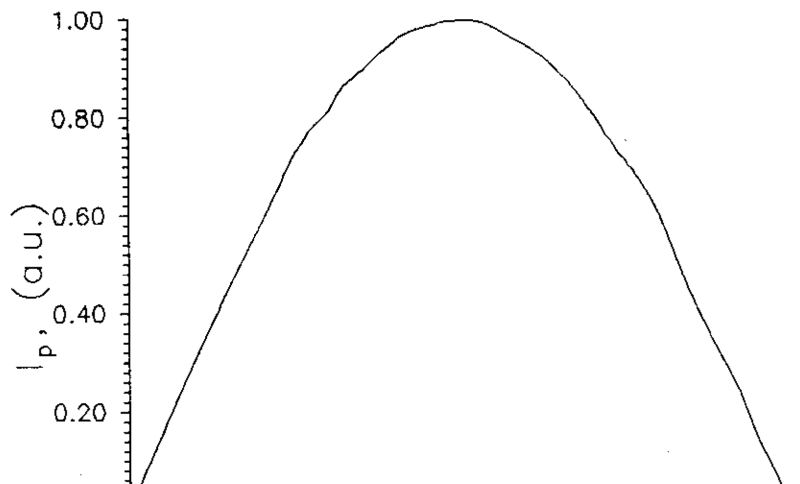

Figure 5. Current-phase relation of BiPbSrCaCuO weak link.

A vector voltmeter was utilized as phase-sensitive detectors to measure the magnitude and phase shift angle of the tank voltage relative to input drive signal. The other parts of the system are typical.

SYSTEM OPERATION

The system operates as follows. The first digital-to-analog converter DAC1 controlled by a computer sets up the control voltage for the dc current supply corresponding the certain dc current I_{DC} (Fig.1). The current I_{DC} determines the external flux Φ_{DC} inside the loop of the SQUID. Then with DAC2 the frequency of the rf-oscillator is changed and the amplitude-to-frequency curve of the tank circuit $L_T C_T$ coupled to the SQUID is investigated. The phase shifter compensates the phase shift in the input curcuit and amplifier. The low pass filter follows the detector. The data sampled with the ADC are stored in the PC for further processing. These measurements are repeated for different external magnetic field Φ_{DC}. The time constant of the low-pass filter is rather big ($5-10$ s) and to decrease the time of measurements we have used the method described in (8). The system is able to measure the phase-dependent quasiparticle current $I_q(\varphi) = G(\varphi)V$, where $G(\varphi) = 1/R(\varphi)-$ is a phase-dependent conductance, V is a voltage across the junction. But usually we have investigated the high$-T_C$ junctions in liquid nitrogen and due to the great noise, there was a considerable error of the measurements, and that is why they have not been carried up.

Fig.4 illustrates the measurement results of the amplitude-to-frequency curves. We have measured a BiPbSrCaCuO weak link embedded in a balk SQUID (10). The results of the calculations is shown in Fig.5. The current-phase relation of this Josephson junction is nearly sinusoidal.

ACKNOWLEDGMENTS

The author would like to express deep gratitude and recognition to Dr.H.Koch for his kind invitation to PTB, where first versions of several system parts were constructed, and for the possibility to use the PTB chips in this work. The author is grateful to Prof.G.Krivoy and Dr.V.Polushkin for helpful discussions and contributions. Dr.Yu.Filippov and Dr.R.Kirschman would be especially thanked for the interest to this research.

REFERENCES

1. D.E.McCumber, J.Appl.Phys., **39**, 3113-3115 (1968).

2. W.S.Stewart, Appl.Phys.Lett., **12**, 277-279 (1968).
3. J.Kurkijärvi, J.Appl.Phys., **44**, 3729 (1973).
4. D.Vincent, B.Deaver, Phys. Rev. Lett., **32**, 212-214 (1974).
5. S.S.Tinchev, Physica C, **222**, 173-175 (1994).
6. V.Polushkin, S.Uchaikin, S.Knappe, H.Koch, B.David, and D.Grundler, was accepted in IEEE Appl. Supercond. in 1994.
7. R.Rifkin, B.S.Deaver, Phys.Rev.B, **13**, 3894-3901 (1976).
8. C.S.Pang, C.M.Falco, and I.K.Schuller, Rev.Sci.Instrum. **51**, 1272-1273 (1980).
9. S.S.DiJulio and E.L.Knuth, Rev.Sci.Instrum. **55**, 1154-1156 (1984).
10. A.V.Blinov, S.V.Uchaikin, Yu.S.Bulyshev, S.V.Serykh, and A.G.Sheider, Superconductivity (USSR), **5**, 1121-1125 (1992).

Received by Publishing Department
on June 5, 1995.